

RED-ACT Report

Real-time Earthquake Damage Assessment using City-scale Time-history analysis

Dec. 19, M5.5 Aomori-ken, Japan Earthquake

Research group of Xinzheng Lu at Tsinghua University (luxz@tsinghua.edu.cn)

First reported at 14:40, Dec. 19, 2019 (Beijing Time, UTC +8)

Acknowledgments and Disclaimer

The authors are grateful for the data provided by **K-NET** and **KiK-net**. This analysis is for research only. The actual damage resulting from the earthquake should be determined according to the site investigation.

Scientific background of this report can be found at: <http://www.luxinzheng.net/rr.htm>

1. Introduction to the earthquake event

At 15:21 19 Dec 2019 (Local Time, UTC +9), an **M 5.5 (JMA)** earthquake occurred in **Japan Aomori-ken**. The epicenter was located at **142.2 40.5**, with a depth of **50.0 km**.

2. Recorded ground motions

16 ground motions near to epicenter of this earthquake were analyzed. The names and locations of the stations can be found Table 1. The maximal recorded peak ground acceleration (PGA) is **251 cm/s/s**. The waveform and corresponding response spectra in comparison with the design spectra specified in the Chinese Code for Seismic Design of Buildings are shown in Figure 1.

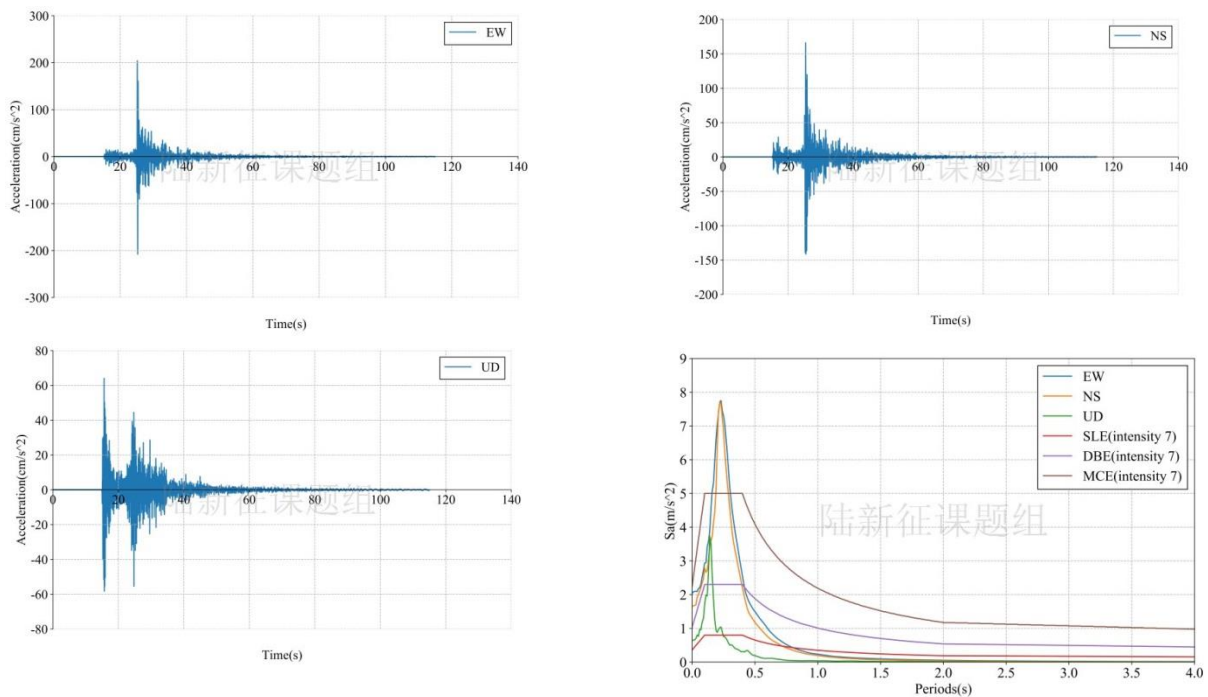


Figure 1 Waveform and response spectra of the recorded ground motions with maximal PGA

3. Damage analysis of the target region subjected to the recorded ground motions

Using the real-time ground motions obtained from the strong motion networks and the **city-scale nonlinear time-history analysis**, the damage ratios of buildings located in different places can be obtained. The building damage distribution and the human feeling distribution near to different stations are shown in Figure 2 and Figure 3, respectively. These outcomes can provide a reference for post-earthquake rescue work

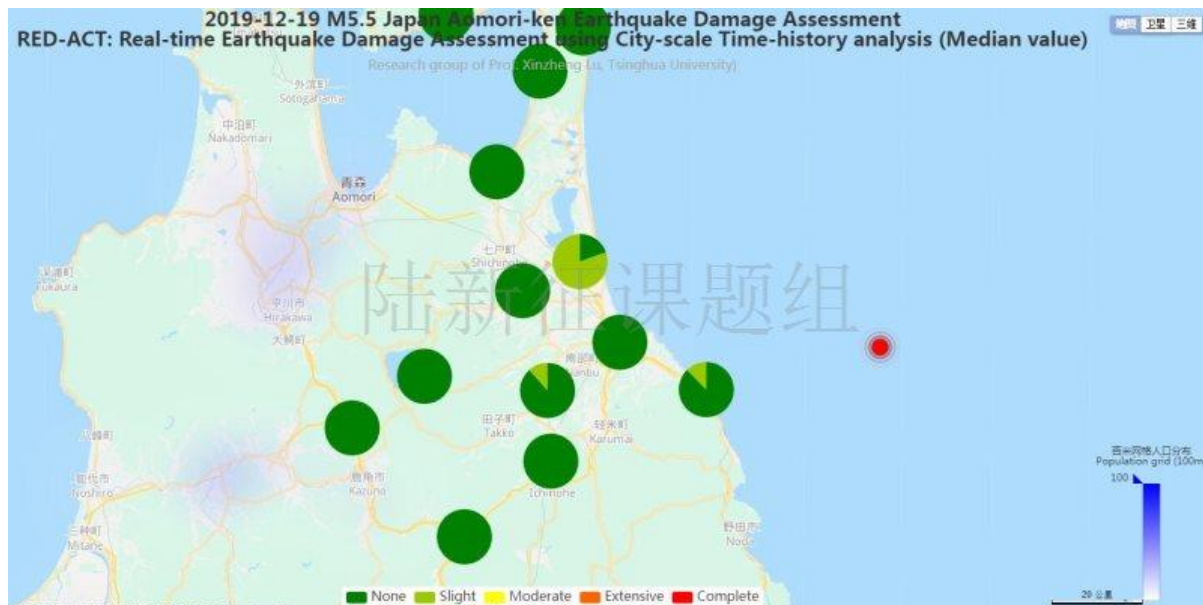


Figure 2 Damage ratio distribution of the buildings near to different stations

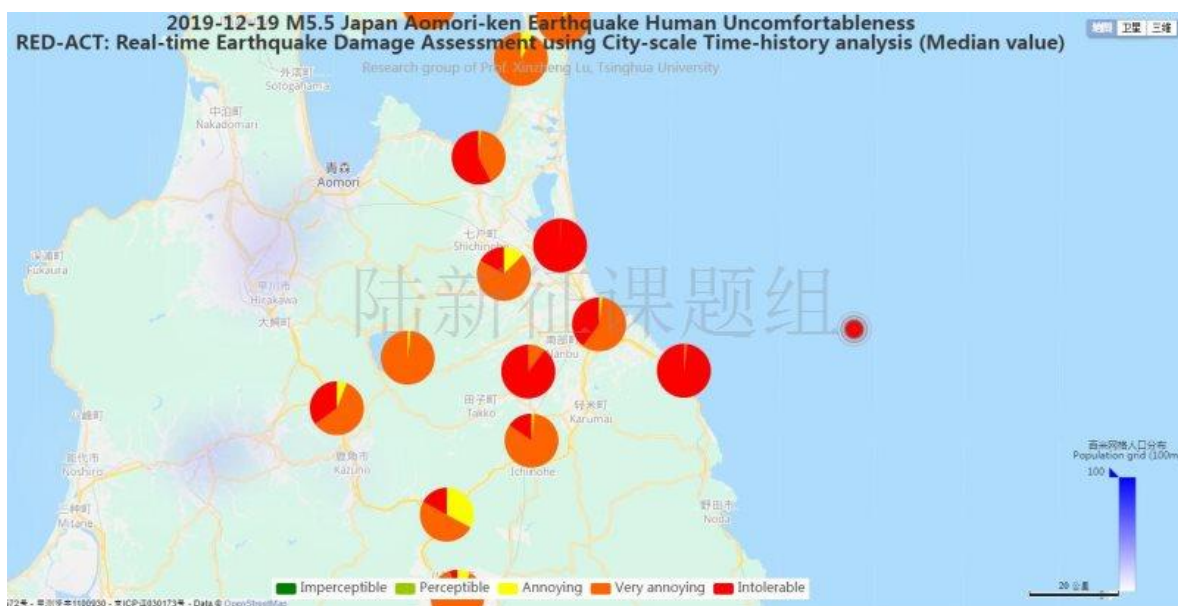
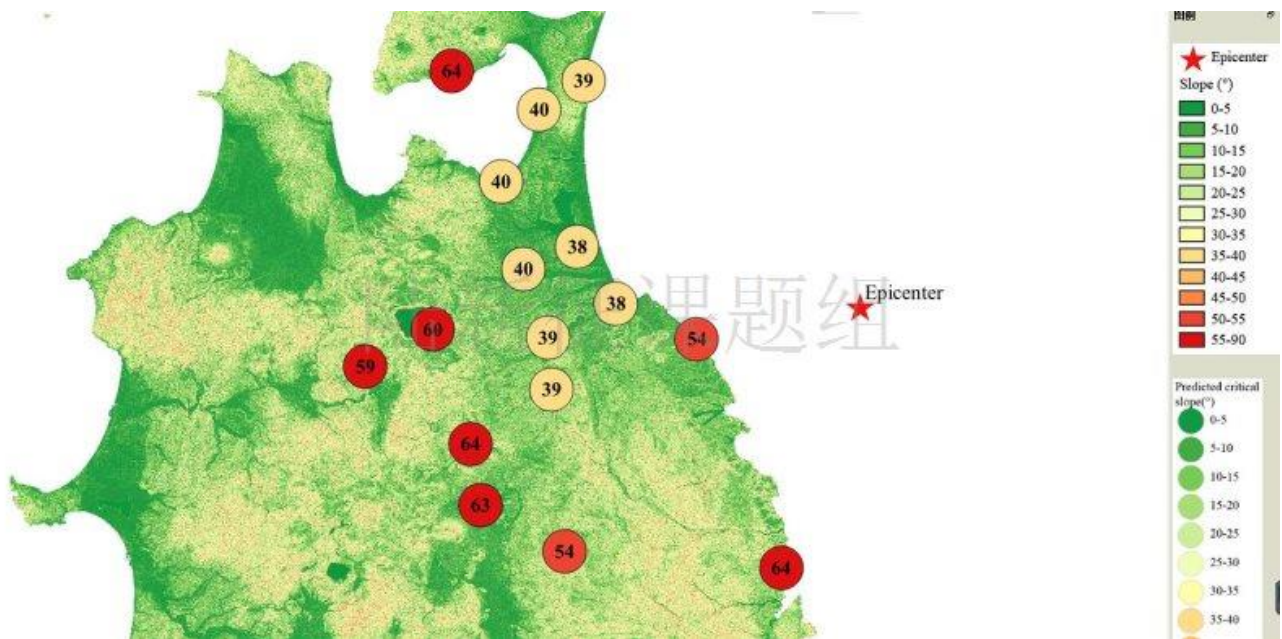


Figure 3 Human feeling distribution near to different stations

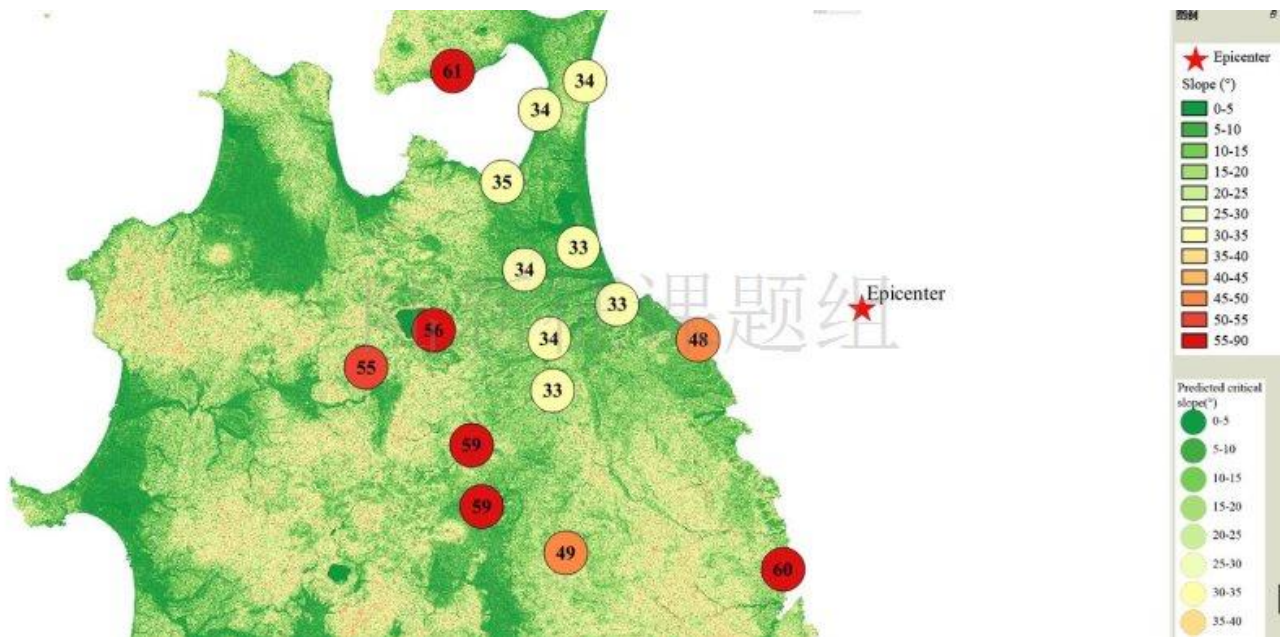
4. Earthquake-induced landslide of the target region subjected to the recorded ground motions

According to local topographic data, lithology data and ground motion records, the distribution of earthquake-induced landslide near to different stations under the different proportions of the landslide slab thickness that is saturated can be calculated, as shown in Figure 4. The basemap shows the distribution of the local

slope. The number in the circle represents the critical slope of the landslide. The earthquake-induced landslide tends to occur with a higher probability when the slope is larger than this threshold value.



(a) The proportion of the landslide slab thickness that is saturated equals 0%



(b) The proportion of the landslide slab thickness that is saturated equals 50%



(c) The proportion of the landslide slab thickness that is saturated equals 90%
 Figure 4 Distribution of earthquake-induced landslide near to different stations

Scientific background of this report can be found at: <http://www.luxinzheng.net/rr.htm>

Table 1 Names and locations of the strong motion stations

No.	Station Name	Latitude	Longitude
1	AKT001	140.743	40.3279
2	AOM006	140.997	41.1976
3	AOM007	141.385	41.169
4	AOM008	141.255	41.084
5	AOM010	141.142	40.8721
6	AOM011	141.367	40.6803
7	AOM012	141.481	40.5138
8	AOM013	141.28	40.4124
9	AOM014	140.941	40.4371
10	AOM021	141.208	40.6152
11	IWT001	141.719	40.4099
12	IWT004	141.967	39.7357
13	IWT020	141.329	39.7841
14	IWT021	141.082	39.9203
15	IWT022	141.052	40.1011
16	IWT024	141.291	40.2612